



---

## Term Paper: PH441

### *Trapped Ion Quantum Computing*

---

S Venkat Bharadwaj 20021045

s.bharadwaj@iitg.ac.in

B.Tech Engineering Physics

Soham Atkar 20021051

a.soham@iitg.ac.in

B.Tech Engineering Physics

DEPARTMENT OF PHYSICS

April 19, 2023

# Contents

<b>1</b>	<b>Introduction</b>	<b>1</b>
<b>2</b>	<b>Ion Trapping</b>	<b>1</b>
<b>3</b>	<b>Qubit Construction</b>	<b>3</b>
3.1	Qubit Initialization and Detection . . . . .	5
<b>4</b>	<b>Implementation of Universal Gates</b>	<b>5</b>
4.1	Single Qubit Gate . . . . .	6
4.2	Cirac-Zoller Gate . . . . .	7
4.3	Molmer-Sorenson Gate . . . . .	9
<b>5</b>	<b>Scalability</b>	<b>11</b>
<b>6</b>	<b>Current Implementations</b>	<b>12</b>
6.1	Honeywell . . . . .	12
6.2	IonQ . . . . .	13
6.3	University of Maryland . . . . .	13
<b>7</b>	<b>Conclusion</b>	<b>13</b>
<b>8</b>	<b>References</b>	<b>14</b>

# Acknowledgement

This academic project was supported by the Indian Institute of Technology Guwahati. We extend our thanks to our Professor Charudatta Kadolkar Sir who provided insight and expertise that greatly assisted the study and motivated us to learn about trapped ion quantum computing and compile our knowledge and passion for the subject into a semester term paper.

## 1 Introduction

The proposal to implement trapped ion systems as a basis for a quantum computer was first proposed by Cirac and Zoller in 1995 through their paper in Physical Review Letters. Fast forward to today and the system is one of the few candidates that satisfies all five general requirements for a quantum computer. Those are:

- Scalable system of defined qubits
- Reliable initialization of qubits
- Long coherence time
- Ability to construct universal gates
- Efficient measurement scheme

Most, if not all, of these requirements have been demonstrated experimentally in such systems. Trapped ion qubits can be categorized based on the energy splitting between the levels used for the qubit architecture. Optical qubits are derived from a ground state and an excited metastable state separated by an optical frequency. On the other hand, the main focus of this term paper is the hyperfine qubit, which is derived from the electronic ground-state hyperfine levels separated by a microwave frequency. Trapped ion computing is a promising new frontier in the field of quantum computing, with many experimental groups worldwide contributing greatly to trapped-ion quantum information processing. Some of these groups are from University of Aarhus, IBM-Almaden, NIST-Boulder, McMaster University, University of Michigan and many more.

## 2 Ion Trapping

While there exist many kinds of ion traps, the Paul trap, based on Radio Frequency, and Penning traps based on DC. Our term paper will be restricting our discussion to linear Paul traps. Now, charged ions feel forces from an electric field, however according to Earnshaw's theorem, it is not possible to confine a charged particle with static electric fields. It is possible to confine a charged ion by a time averaged force, wherein the electric fields switch between confining directions and anti-confining directions at a rate that is faster than the time an ion can take to escape the field, this generally done at frequencies at the order of radio waves, hence the name. This is often done with the help of a

quadrupole geometry as shown in Figure 1.

We can begin to characterize the linear RF trap with the help of a schematic diagram

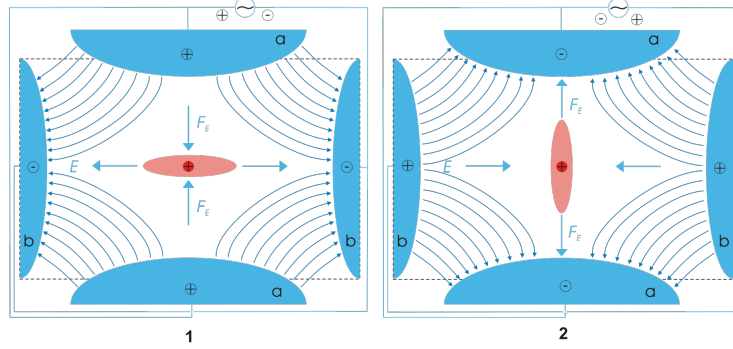


Figure 1: Scheme of a Quadrupole ion trap of classical setup with a particle of positive charge (dark red), surrounded by a cloud of similarly charged particles (light red). The electric field  $E$  (blue) is generated by a quadrupole of endcaps (a, positive) and a ring electrode (b)

shown in figure 2. Essentially, the ions become bound by a ponderomotive potential  $U_{x,y}$  given by:

$$U_{x,y}(\mathbf{r}) = \frac{q^2}{2m\Omega_T^2} \langle E^2(\mathbf{r}) \rangle$$

which can be approximated to:

$$U_{x,y}(\mathbf{r}) \cong \frac{q^2 V_0^2}{4m\Omega_T^2 R^4} (x^2 + y^2)$$

Where  $q$  is the ion's charge,  $m$  is it's mass and  $E$  is the RF electric field that is applied as a result of the pseudopotential  $V_0 \cos(\Omega_T t)$  that is applied to the dark shaded electrodes in figure 2.  $\mathbf{r}$  is the radial distance from the primary axis and  $R$  is the radial distance between the primary axis of the trap and the nearest electrode surface. The configuration yields a an ion oscillation frequency given by:

$$\omega_{x,y} \simeq \frac{qV_0}{\sqrt{2}\Omega_T m R^2}$$

The pseudopotential makes use of the following assumptions:  $\omega_{x,y} \ll \Omega_T$  and  $\omega_z \ll \omega_{x,y}$  so that the static radial forces can be ignored when compared to the pseudopotential forces. We can say that the ions would tend towards the region of minimum  $|E(\mathbf{r})|$  from the above expressions. From the perspective of quantum computing, it is reasonable to assume the linear trap as a 3-dimensional harmonic oscillator well for qubits where the strength of the well is much stronger along the  $x$  and  $y$  axes as compared to the  $z$  axis. Each ion would tend towards the bottom of the well but due to the mutual Coulombic interactions, these ions would arrange themselves in an array-like configuration at equilibrium. Two ions in the array are spaced by  $2^{1/3}d$  whereas three ions would be spaced by  $(5/4)^{1/3}d$ , here  $d$  is the spacing parameter given by:

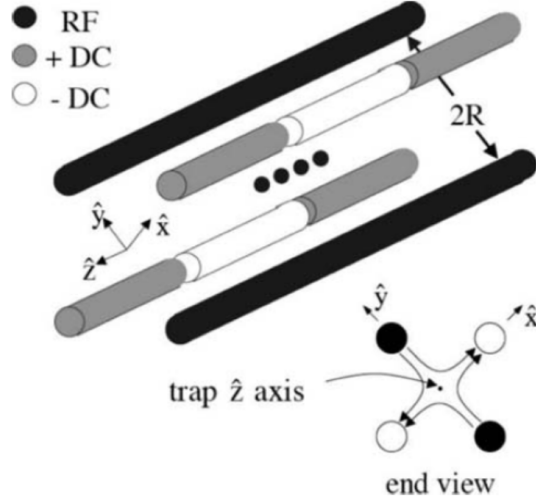


Figure 2: Electrode configuration for a linear RF (Paul) trap. A common RF potential  $V_0 \cos(\Omega_T t)$  is applied to the dark electrodes; the other electrodes are held at RF ground through capacitors (not shown) connected to ground. The lower-right portion of the figure shows the x, y electric fields from the applied RF potential at an instant when the RF potential is positive relative to ground. A static electric potential well is created (for positive ions) along the z-axis by applying a positive potential to the outer segments (grey) relative to the center segments (white).

$$d(\mu m) = \frac{15.2}{(M(amu)v_z^2(MHz))^{1/3}}$$

While it is possible to demonstrate simple gate operations, in order to construct a viable, scaled quantum computer we must drastically increase the number ions in the trap to make sure there are sufficient qubits for the computer architecture. However, this leads to several difficulties. With the addition of each ion, three vibrational modes are added to the array. That means that it would be impossible to spectrally select the desired vibrational modes with the desired optimum operation speed. On top of that, since every large processor will have to incorporate error correction, it would be desirable to have a system where the ancilla qubits can be reset without affecting the logical qubits' coherence. Laser scattering is typically used to reset qubits in ion traps, the scattered light from which may decohere the logical qubits in the system. However, linear traps are advantageous due to increased ion storage capacity, faster scan times, and simplicity of construction.

### 3 Qubit Construction

The ions in an ion trap can be confined for days in the ultra-high vacuum with very little perturbations to the atomic structure. This makes certain internal states in the atom ideal for qubit construction. As the ions experience a vanishing time-averaged electric field, the perturbations from it are negligible. While the magnetic field perturbations

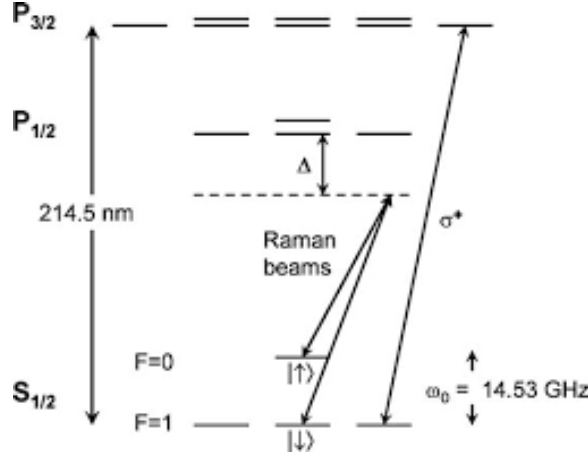


Figure 3: Electronic energy levels of the  $^{111}\text{Cd}^+$  ion. The  $^2S_{1/2}$  ( $F = 1, m_F = 0$ ) and  $^2S_{1/2}$  ( $F = 0, m_F = 0$ ) hyperfine ground states (denoted by  $|\downarrow\rangle$  and  $|\uparrow\rangle$  respectively), separated in frequency by  $\omega_{HF}/2\pi \simeq 14.53$  GHz, and magnetic field insensitive to first order, form the basis of a quantum bit. Detection of the internal HF state is accomplished by illuminating the ion with a  $\sigma^+$ -polarized “detection” beam near  $\lambda_{Cd} \simeq 214.5$  nm and observing the fluorescence from the cycling transitions between  $|\downarrow\rangle$  and the  $^2P_{3/2}$   $|(F = 2, m_F = 2)\rangle$  state. The excited P state has radiative linewidth  $\gamma_e/2\pi \simeq 47$  MHz. Also drawn are a pair of  $\sigma^+$ -polarized Raman beams that are used for quantum logic gates.

will affect the internal states, we can make the coherence between two internal states insensitive to the magnetic field (to the lowest order). This can be achieved by operating near the extremum of the energy separation between the two intrinsic levels with respect to the magnetic field. Qubit coherence has been observed last upto times far exceeding 10 minutes in such atomic ground states.

Trapped ions can host qubits by storing them in metastable states separated by optical frequencies which would undergo simple, single-photon transitions, provided that the decay rate is sufficiently low (certain atomic ions have lifetimes  $\gg 1$  s). For such optical states, phase-stable narrow linewidth laser are required in order to truly realize the benefits of the long decay times. Additionally, Stark shifts from coupling to non-resonant allowed transitions are required for longer lifetimes as we would need a laser with a high intensity in order to obtain significant transition rates.

Long radiative lifetimes can be found in ground state hyperfine levels, which are typically separated by frequencies of the order of microwaves. This makes trapped ion hyperfine levels arguably the most suitable system for constructing qubit states. Let us consider the  $^{111}\text{Cd}^+$  ion whose energy level diagram is displayed in figure 3. The two primary states of interest will be the  $^2S_{1/2}$  ( $F = 1, m_F = 0$ ) and  $^2S_{1/2}$  ( $F = 0, m_F = 0$ ) hyperfine ground states (represented by  $|\downarrow\rangle$  and  $|\uparrow\rangle$  respectively). These two levels are separated by a frequency  $\omega_{HF}$  where  $\omega_{HF}/2\pi \simeq 14.53$  GHz for  $^{111}\text{Cd}^+$  ions. These long lifetime spin states will form the basis of the qubit states for a trapped-ion HF quantum computer. There are other systems with similar advantages and can serve as hosts for qubits such as  $^9\text{Be}^+$ ,  $^{25}\text{Mg}^+$ ,  $^{43}\text{Ca}^+$ ,  $^{87}\text{Sr}^+$ ,  $^{137}\text{Ba}^+$  and  $^{199}\text{Hg}^+$ .

### 3.1 Qubit Initialization and Detection

We can initialize HF qubits into either  $|\uparrow\rangle$  or  $|\downarrow\rangle$  states with the aid of standard optical pumping techniques. We can detect the spin states with the help of quantum jumps. Inducing an RF signal between different eigenstates in the ion trap system results in quantum jumps between these states which can be analyzed by resonance fluorescence. To demonstrate considering the case of the  $^{111}\text{Cd}^+$  ion, a circularly polarized laser beam resonant with the  $^2S_{1/2} \rightarrow ^2P_{3/2}$  transition at  $\lambda \simeq 214.5$  nm scatters photons if it is in the  $|\uparrow\rangle$  state but essentially no photons are scattered if it is in the  $|\downarrow\rangle$  state. Even if a modest number of photons are scattered, the efficiency in being able to distinguish them is about 100%. Generally, the efficiency in detecting HF qubits with a cycling transition between the two states is given by:

$$\eta = 1 - \left(\frac{M}{\epsilon_{\text{photon}}}\right)\left(\frac{\gamma_e}{\omega_{HF}}\right)^2$$

where  $M$  factors in atomic branching ratios and is of the order of unity, and  $\epsilon_{\text{photon}}$  is the photon detection efficiency of the ion fluorescence. Once again, consider the  $^{111}\text{Cd}^+$  ion, figure 4 plots a histogram/frequency distribution of the number of photons detected in 0.2 ms. The net quantum efficiency is  $\sim 10^{-3}$  and the histogram is plotted for both bright ( $|\uparrow\rangle$ ) and dark ( $|\downarrow\rangle$ ) states.

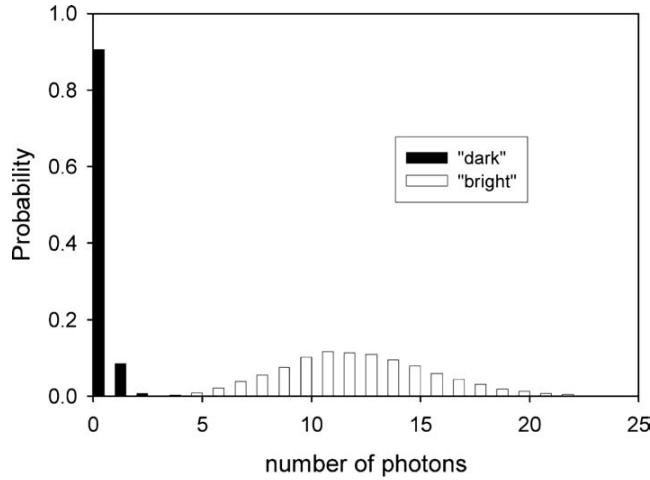


Figure 4: Detection histograms of a single trapped  $^{111}\text{Cd}^+$  ion. The white bars correspond to the distribution of the number of fluorescence photons detected by a CCD camera for a  $^{111}\text{Cd}^+$  ion prepared initially in the  $|\downarrow\rangle$  state upon application of a  $\sigma^+$ -polarized detection laser for 0.2 ms. The black bars correspond to the photon distribution for the ion initially prepared in the  $|\uparrow\rangle$  state under the same conditions. The very small overlap between the two distributions corresponds to a detection efficiency of  $>99.7\%$ .

## 4 Implementation of Universal Gates

Universality on computation refers to a machine that is capable of performing any and every possible physical calculation. In terms of a classical computer, if a machine can

take any string of binary input and convert it into any arbitrarily chosen string, we call it universal. Although the proof is extremely difficult and technical, it is known that a machine capable of performing the basic logical operations (AND, OR, NOT) is universal. Universal gates are the basic components that are used to construct these basic operations. For a classical computer, it is shown that NAND and NOR gates universal.

Similarly for a quantum computer, universality refers to the ability to achieve any desired rotation (change in state) on any arbitrary number of qubits. Thus, universality is achieved when we are able to manipulate the state of each qubit independently (unitary rotation) and we can entangle 2 different qubits (here ions). One such gate that can entangle two different qubits is the Controlled-NOT (CNOT) gate.

The CNOT gate acts just like the name suggests. It acts on 2 bits - one for the control and the other the target. If the control bit is in the basis state  $|0\rangle$ , the target bit is unchanged and if the control bit is in the basis state  $|1\rangle$ , then the target becomes the complement of itself. It's matrix representation is given as

$$CNOT = \begin{pmatrix} 1 & 0 & 0 & 0 \\ 0 & 0 & 0 & 1 \\ 0 & 0 & 1 & 0 \\ 0 & 1 & 0 & 0 \end{pmatrix}$$

$$CNOT |0\rangle \otimes |0\rangle = |00\rangle = |0\rangle \otimes |0\rangle$$

$$CNOT |1\rangle \otimes |0\rangle = |11\rangle = |1\rangle \otimes |1\rangle$$

An entangled state of these 2 qubits can be achieved when the control bit is not in a basis state rather in a linear combination of them. Acting a Hadmard gate on the control bit (which is initially in a basis states), then acting a CNOT gate generates maximally entangled 2 qubit states known as bell states.

$$\Psi = H |0\rangle = \frac{|0\rangle + |1\rangle}{\sqrt{2}}$$

$$CNOT \Psi \otimes |0\rangle = \frac{|00\rangle + |11\rangle}{\sqrt{2}} \neq \Psi \otimes \Psi'$$

The basic principle of gates in the trapped ion Quantum computing is the use of laser focusing on one/multiple atoms to bring about excitation and de-excitation in the atom, thus changing the state of the system. In this section, we will see some of the implementations of this to make the universal gates.

## 4.1 Single Qubit Gate

Rotation of the qubit states can be achieved by applying microwave radiation of appropriate wavelength corresponding to the energy between excited and ground state of the ion.



Low gain microwave horns are useful tools to generate strong beam of Microwave. Thus, by using such clean sources, one can make a joint rotation of all the qubits. However, for a single ion rotation, one would need to couple radiation of the order of  $10^{-2}\text{m}$  with an ion trap ( $< 10^{-3}\text{m}$ ). Thus addressing individual atoms with it is difficult.

Generally single qubit rotations are implemented by driving Stimulated Raman Transitions (SRT) with 2 laser fields that are properly detuned from an excited state. In this method, two co-propagating laser fields are applied to the ion, each with a detuning  $\Delta \gg \gamma_e$  from an excited state  $|e\rangle$ , with radiative linewidth  $\gamma_e$ . The frequency difference in the 2 fields is set to the frequency corresponding to the energy between excited and ground state of the ion. This results in a coherent field that rotates the qubit similar to microwaves. However, these lasers can be focused on individual ions. The SRT Rabi frequency is given by  $\Omega = \frac{g_1 g_2^*}{\Delta}$ , where  $g_i$  are the resonant Rabi frequencies of the 2 lasers. The Hamiltonian for this interaction is given as

$$\hat{H}_n = \frac{\Omega}{2} [|e\rangle_n \langle g| a e^{-i\phi} + |g\rangle_n \langle e| a^\dagger e^{i\phi}]$$

and the time evolution operator for interaction time  $t_o = \frac{k\pi}{\Omega}$  is given by

$$\hat{V}_n^k(\phi) = e^{-i\hat{H}_n t_o} = \exp[-ik \frac{\pi}{2} (|e\rangle_n \langle g| a e^{-i\phi} + |g\rangle_n \langle e| a^\dagger e^{i\phi})]$$

The probability of spontaneous emission from off-resonant excitation during SRT pulse goes as  $P_{se} = \frac{\gamma_e}{\Delta}$ . Larger the  $\Delta$ , smaller the probability of SE. However, we cannot increase  $\Delta$  indefinitely. We have to select ion candidates such that the excited state life time is sufficient.

## 4.2 Cirac-Zoller Gate

As we have already seen, the ions have been laser cooled in all dimensions so that they undergo very small oscillations around the equilibrium. In such a case, the ions can be described in terms of normal modes. When a laser beam acts on one of the ions, it induces transition between its ground state and excited states and also changes the state of the collective normal modes, thus affecting the whole system. However, in Lamb-Dicke limit and for sufficiently low intensities, it will only cause transitions that modifies the state of one such normal mode.

With a laser frequency such that its detuning equals minus of the Center of Mass (CM) mode, one excites the CM mode exclusively. Consider laser acting on the  $n^{th}$  ion. This laser will not affect the internal states of the other ions. The laser frequency is chosen such that the equilibrium position of the ion corresponds to node in the laser standing wave. In such a case, the Hamiltonian (in the Lamb-Dicke limit) is given by,

$$\hat{H}_{n,q} = \frac{\eta}{\sqrt{N}} \frac{\Omega}{2} [|e_q\rangle_n \langle g| a e^{-i\phi} + |g\rangle_n \langle e_q| a^\dagger e^{i\phi}]$$

where,  $\Omega$  is the Rabi frequency,  $a$ ,  $a^\dagger$  are the creation and annihilation corresponding to the CM Phonon,  $\eta$  is the LDL parameter that depends on wave vector and direction of propagation of laser, the subscript  $q$  refers to transition excitation, that depends on laser polarisation. For a certain time  $t_o = \frac{k\pi\sqrt{N}}{\Omega\eta}$  (i.e. a  $k\pi$  pulse), the time evolution operator is given by,

$$U_{q,n}^k = e^{-i\hat{H}_q t_o} = \exp[-ik\frac{\pi}{2}(|e_q\rangle_n \langle g| a e^{-i\phi} + |g\rangle_n \langle e_q| a^\dagger e^{i\phi})]$$

Using this interaction, one can perform a 2-bit gate by following these steps:

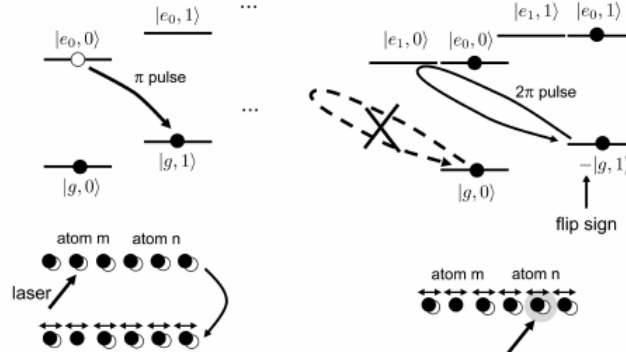


Figure 5: Step i) and ii) for implementing CZ Gate

- i) A  $\pi$  pulse laser on  $m^{th}$  ion with polarisation  $q = 0$  and  $\phi = 0$ .
- ii) A  $2\pi$  pulse laser on  $n^{th}$  ion with polarisation  $q = 1$  and  $\phi = 0$ . The different polarization is useful for rotating the qubit through an auxillary state.
- iii) A  $\pi$  pulse laser on  $m^{th}$  ion with polarisation  $q = 0$  and  $\phi = 0$ .

The effect of these is shown below:

$$U_{0,m}^1 U_{1,n}^2 U_{0,m}^1 |g\rangle_m |g\rangle_n |0\rangle \rightarrow U_{0,m}^1 U_{1,n}^2 |g\rangle_m |g\rangle_n |0\rangle \rightarrow U_{0,m}^1 |g\rangle_m |g\rangle_n |0\rangle \rightarrow |g\rangle_m |g\rangle_n |0\rangle$$

$$U_{0,m}^1 U_{1,n}^2 U_{0,m}^1 |g\rangle_m |e_0\rangle_n |0\rangle \rightarrow U_{0,m}^1 U_{1,n}^2 |g\rangle_m |e_0\rangle_n |0\rangle \rightarrow U_{0,m}^1 |g\rangle_m |e_0\rangle_n |0\rangle \rightarrow |g\rangle_m |e_0\rangle_n |0\rangle$$

$$U_{0,m}^1 U_{1,n}^2 U_{0,m}^1 |e_0\rangle_m |g\rangle_n |0\rangle \rightarrow U_{0,m}^1 U_{1,n}^2 -i |g\rangle_m |g\rangle_n |1\rangle \rightarrow U_{0,m}^1 i |g\rangle_m |g\rangle_n |1\rangle \rightarrow |e_0\rangle_m |g\rangle_n |0\rangle$$

$$U_{0,m}^1 U_{1,n}^2 U_{0,m}^1 |e_0\rangle_m |e_0\rangle_n |0\rangle \rightarrow U_{0,m}^1 U_{1,n}^2 -i |g\rangle_m |e_0\rangle_n |0\rangle \rightarrow U_{0,m}^1 -i |g\rangle_m |e_0\rangle_n |0\rangle \rightarrow -|e_0\rangle_m |e_0\rangle_n |0\rangle$$

A Controlled NOT gate can be constructed with addition of appropriate single rotation operator in  $n^{th}$  qubit.

$$CNOT_{m,n} = V_n^{1/2}(\pi/2) U_{0,m}^1 U_{1,n}^2 U_{0,m}^1 V_n^{1/2}(-\pi/2)$$

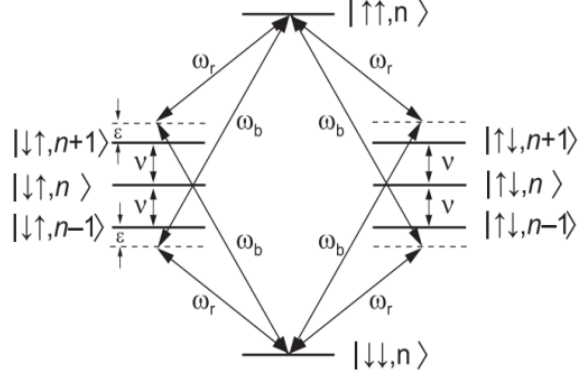


Figure 6: Atomic State Diagram for MS Gate

### 4.3 Molmer-Sorenson Gate

In a CZ gate, the trapped ions coupled with the vibrational excitation state and ground state, and irradiation of a second ion, couples them together. In 2000, Molmer-Sorenson proposed application of bichromatic light which selects certain excited intermediate states, and thus desired internal state of the ions is achieved. Ions in a linear trap interacting with a laser field of frequency  $\omega$  is described by the Hamiltonian

$$\begin{aligned}\hat{H} &= \hat{H}_o + \hat{H}_{int} \\ \hat{H}_o &= \nu a^\dagger a + 1/2 + \omega_{eg} \sum_i \sigma_{zi}/2 \\ \hat{H}_{int} &= \sum_i \frac{\Omega}{2} (\sigma_{+i} e^{\eta_i(a+a^\dagger) - \omega t} + hc)\end{aligned}$$

where,  $\nu$  is the normal mode frequency,  $a^\dagger$  and  $a$  are the annihilation and creator operators of the oscillator,  $\omega_{eg}$  is energy difference b/w excited state,  $e$  and ground state,  $g$ ,  $\Omega_i$  is the resonance Rabi frequency,  $\eta$  is LDL factor.

In this scheme, we choose the detuning of the laser addressing the first ion close to the upper sideband, i.e. close to resonance with a joint vibrational and internal excitation of ion. For the laser addressing the second ion, we choose detuning equal to the negative of detuning for the first ion. This laser setting couples the states  $|g\rangle_1 |g\rangle_2 |n\rangle \rightarrow [|e\rangle_1 |g\rangle_2 |n+1\rangle, |g\rangle_1 |e\rangle_2 |n-1\rangle] \rightarrow |e\rangle_1 |e\rangle_2 |n\rangle$  (where  $n$  is the vibrational mode). By keeping the detuning from sideband large enough, we can make sure the intermediate states are not populated.

Assuming the rabi frequency and LDL factor of both ions are same, in the weak field regime, we can calculate Rabi frequency for the transition  $\tilde{\Omega}$  using second order perturbation theory,

$$\frac{\tilde{\Omega}^2}{2} = \sum_m \frac{\langle e e n | H_{int} | m \rangle \langle m | H_{int} | g g n \rangle}{E_{g g n} + \omega_i - E_m}$$

Restricting the sum to intermediate states  $[|e\rangle_1 |g\rangle_2 |n+1\rangle, |g\rangle_1 |e\rangle_2 |n-1\rangle]$ , we get,

$$\tilde{\Omega} = -\frac{(\Omega\eta)^2}{2(\nu - \delta)}$$

where,  $\delta$  is the detuning frequency for ion 1.

The final expression for the Rabi frequency is independent of  $n$ , which implies that the evolution of inter-atomic states are insensitive to the vibrational mode. From the above arguments, and numerical solution of the Schrodinger equation by Sorenson and Molmer, The final states for interaction time  $T$  is given by,

$$\begin{aligned} |gg\rangle &\rightarrow \cos\left(\frac{\tilde{\Omega}T}{2}\right) |gg\rangle + i \sin\left(\frac{\tilde{\Omega}T}{2}\right) |ee\rangle \\ |ee\rangle &\rightarrow \cos\left(\frac{\tilde{\Omega}T}{2}\right) |ee\rangle + i \sin\left(\frac{\tilde{\Omega}T}{2}\right) |gg\rangle \\ |ge\rangle &\rightarrow \cos\left(\frac{\tilde{\Omega}T}{2}\right) |ge\rangle - i \sin\left(\frac{\tilde{\Omega}T}{2}\right) |eg\rangle \\ |eg\rangle &\rightarrow \cos\left(\frac{\tilde{\Omega}T}{2}\right) |eg\rangle - i \sin\left(\frac{\tilde{\Omega}T}{2}\right) |ge\rangle \end{aligned}$$

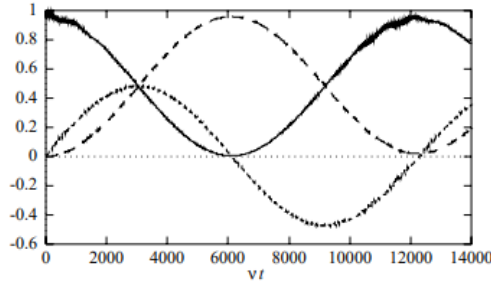


FIG. 2. Rabi oscillations between  $|gg\rangle$  and  $|ee\rangle$ . The figure shows the time evolution of the internal atomic density matrix elements  $\rho_{gg,gg}$  (full line),  $\rho_{ee,ee}$  (long-dashed line), and  $\text{Im}(\rho_{gg,ee})$  (short-dashed line). The magnitude of  $\text{Re}(\rho_{gg,ee})$  is below 0.03 and is not shown. In the initial state, the ions are in the internal ground state and a coherent vibrational state with mean excitation  $\bar{n} = 2$ . Parameters are  $\delta = 0.90\nu$ ,  $\Omega = 0.10\nu$ , and  $\eta = 0.10$ .

Figure 7: Numerical Solution from Molmer et al.

Implementation of CNOT Gate:

$$CNOT_{1,2} = P_1 P_2^{-1} H_2 R P_1 H_1 P_1 R P_2$$

where,  $P_i$  corresponds to  $\pi/2$  phase change on ion  $i$ ,  $H$  corresponds to Hardmard on ion  $i$ ,  $R$  corresponds to MS gate with  $t = \pi/2\tilde{\Omega}$

The major improvements of MS gate over CZ gates are:

- The ions need not be in the ground state initially.
- Entanglement can be achieved through a single step.
- Individual ion laser beam focusing is not required.

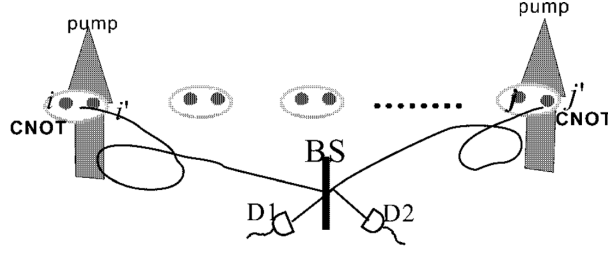


Figure 8: Schematic illustration of computation based on probabilistic photon-mediated entanglement between separated ions

## 5 Scalability

As mentioned earlier in the Ion Trapping section, a large number of ions in the RF trap leads to certain issues when trying to scale up the system. Therefore, in order to construct scalable ion trap quantum computers, novel systems must incorporate arrays of interconnected traps, with only a few ions in each array. Information can be carried between arrays in two ways:

- **Photons:** A series of ion pairs, each in distinct trap arrays are separated by an arbitrary distance. Each qubit consists of a logic and ancilla ion. To achieve scalability, we could perform deterministic quantum gates between two logic ions in different pairs. Each ancilla ion could be connected to a single photon detector. In order to entangle them, we could pump both ancilla ions to excited electronic states with a resonant laser beam. From the resulting spontaneously emitted photons will be directed to single-photon detectors for a Bell-type collective measurements. For a certain measurement, two ancilla ions will be projected onto a Bell state. We assume that the logic and ancilla ions are sufficiently spectrally resolved so that the entanglement operation on the ancilla ions does not influence the logic ions. The schematic for the same is outlined in figure 8.
- **Ions:** Certain strategies demand a "head" ion held in a movable trap to carry information from site-to-site. Or, qubit ions themselves could be shuttled in between an array of interconnected traps. Here, ions would be moved between nodes in the array by applying time-dependent potentials to "control" certain segments. Logic operations between select ions could be done by transferring them to a trap that is a de-facto accumulator. Subsequently, these ions are moved to memory locations or other accumulators. This technique maintains fewer motional modes that need to be accounted and minimizes the issue of ion-laser-beam addressing using focused laser beams. These arrays also enable highly parallel processing and ancilla qubit readout in a designated trapping region such that the logical ions are shielded from the scattered laser light. A schematic layout is presented in figure 9.

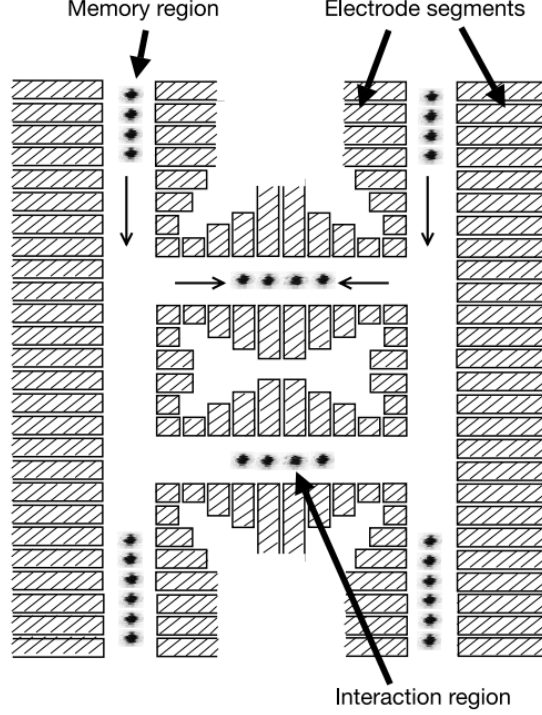


Figure 9: Schematic layout of an extended ion trapped charge coupled device. Ions are stored in the memory region and moved to the interaction region for logical operations. The thin arrows show the transport directions and confinement along the primary trap axis.

## 6 Current Implementations

With the development of Ion trap physics, and the improving implementations of the universal gates with much higher fidelity, Ion trap quantum computers have a lot of promise. At present some of the state of the art implementations of Ion Trap computers are:

### 6.1 Honeywell

Honeywell is a technological based MNC that is headed in the US. Its H1 quantum computer is a 10-qubit ion trap QC that uses Ytterbium ions as qubits. It operates at the temperature of milli-Kelvin. They have achieved a quantum volume of 1024. This system boasts a high fidelity rate of 99.99% for single qubits and 99.84% for 2 qubit gates. Using this system, they have been able to demonstrate the Grover's Algorithm. They were also able to factor 15 into 3 and 5. They have also successfully simulated 32 spin system using the chaotic dynamics of kicked Ising model.

## 6.2 IonQ

IonQ is a quantum computing start up that has been able to successfully develop 32 bit Ion trap quantum computer (Forte and Aria). These system also operate at 10 milli-Kelvin and are based on Ytterbium ions that are held in place by a series of EM fields. They have been able to achieve fidelity rates of 99.97% for single qubit and 99.43% for 2 qubit gates. Thus far, they have used their computer to simulate electronic structures of molecules. They have also been delving in the fields of ML and optimization, and have been able to solve Travelling Salesman Problem for upto 6 cities.

## 6.3 University of Maryland

UMD is one of the top researcher institutes in the field of quantum computing research. One of their most notable implementations in the Trapped Ion Quantum Information Processor. It consists of a 2D array of ion traps with 10 ion traps. Ion traps can be added or removed based on their requirements in this system. They use Beryllium ions and are capable of performing quantum gates and algos on upto 10 qubits using a combination of laser and microwave radiation. Another notable system is their Microfabricated Ion Trap. It is a compact ion trap that allows for precise control and manipulation of trapped ions.

## 7 Conclusion

In this paper, we have seen the principles behind the implementation of an ion trap quantum computer. It passes all 5 of Di Vincenzo's criteria i.e Qubit initialization, Single Qubit Measurement, Universality, Coherence Time, Scalability. Due to the fact that ions can be trapped and manipulated with great control, we have been able to achieve high level of precision and accuracy through ion trap quantum computing. However, there are still many challenges to overcome in order to scale up this system to a level where we can use it for practical applications. Despite these challenges many technological companies and institutions are researching on making these computers more practical and feasible. In the end, eventhough these computers do not seem to be practical, they are very important research topics and development in quantum computing has the potential to transform not just computing but various other fields as well and Ion Trap Quantum Computers with its wide success might be one of the best method of implementation of a Quantum Computer.

## 8 References

- Trapped Ion Quantum Computer Wiki
- Trapped Ion Hyperfine Qubits
- How to build a Quantum Computer
- Ion Trapped Quantum Computer PennyLane
- Overview of Quantum Gates in Ion Trapped Quantum Computers
- Universality
- Entanglement and quantum computation with ions in thermal motion
- Quantum Computations with Cold Trapped Ions
- Honeywell H1
- IonQ Forte
- Photon mediated scaled quantum architecture
- Ion mediated scaled quantum architecture
- Quantum Jumps